Theoretical Valence Photoelectron and UV-visible Absorption Spectra of Four Stable Conductive Molecules Obtained by MO Calculations

Kazuchiyo Takaoka, Sigehiro Maeda, Hidetoshi Miura, Takao Otsuka,† Kazunaka Endo,*,† and Delano Pun Chong*,††

Research Center, Mitsubishi Paper Mills Ltd., 46 Wadai, Tukuba 300-4247

†Department of Chemistry, Faculty of Science, Kanazawa University, Kakuma-machi, Kanazawa 920-1192

††Department of Chemistry, University of British Columbia, 2036 Main Mall, Vancouver, B. C. Canada V6T 1Z1

(Received July 5, 1999)

Theoretical valence photoelectron and UV-visible absorption spectra of four stable conductive molecules (*N*, *N*′-diphenyl-1,4-phenylenediamine (DPPD), *p*-quaterphenyl (PQP), 2, 3, 7, 8, 12, 13, 17, 18-octaethyl-21*H*, 23*H*-porphyrin (OEP), and 29*H*, 31*H*-phthalocyanine (PC)) have been obtained by semiempirical HAM/3 and ZINDO MO calculations, respectively. The Al $K\alpha$ photoelectron spectra were simulated using Gaussian lineshape functions of an approximate linewidth 0.10 E_k ($E_k = E'_k - \mathrm{WD}$), where E'_k is the vertical ionization potential (VIP) of each MO and WD is a shift to account for sample work function and other energy effects, as stated in previous studies. The theoretical valence spectra of the four conductive compounds are in good accordance with the observed ones. The theoretical UV-visible absorption curves of DPPD, PQP, OEP, and PC were obtained after AM1 calculations with COSMO option to reflect solvent effects. The absorption curves as simulated with Gaussian lineshape functions of a constant linewidth of 0.003 eV. Correspond well to the observed spectra. For PC, the simulated spectrum which consists of 0.5 inner protonation (IP) and 0.5 outer protonation (OP) types for PC-ring shows much better agreement with the experimental spectrum in H_2SO_4 than the spectrum of either IP or OP type alone.

We are interested in conductive molecules (*N*, *N*′-diphenyl-1,4-phenylenediamine (DPPD), *p*-quaterphenyl (PQP), ((2, 3, 7, 8, 12, 13, 17, 18-octaethyl-21*H*, 23*H*-porphyrin (OEP), and metal-free phthalocyanine (PC)) industrially in order to design dyes, organic photo-conductors, and organic catalysts. Part of the interest in DPPD as an oligomer of polyaniline[1,2] and PQP comes from a generic relationship to the conductive materials.[3,4] OEP and PC are well-known as dyes and photo-sensitive compounds. PC is applied to the laser organic photo-conductor plate as a electro-photographic material.[5] OEP and PC have attracted much attention because of their remarkable roles in biological redox processes.[6,7] We think that it would be a very useful step in the design of new organic conductive or photosensitive materials to examine the electronic state of the four molecules from theoretical and experimental viewpoints.

For PC compounds, experimental and theoretical fundamental studies were performed by several investigators.[8—12] Berkowitz,[8] and Edwards and co-worker[9] obtained experimental valence ultraviolet photoelectron spectra (UPS) and UV-visible spectra of PC in gas phase, respectively. Orti and co-worker[10] simulated the valence XPS by Koopmans' theorem using valence effective Hamiltonian (VEH) calculations. The energy scale of the simulated spectra had to be contracted for a good fit with the observed spectrum. Kobayashi and co-worker[11] analyzed the visible absorption spectra of PC and the metal-PC using Pariser–Parr–Pople (PPP) SCF MO method. Recently, Toyota, Hasegawa, and Nakatsuji[12] performed the first accurate ab initio study of excited states of free base phthalocyanine by the symmetry-adapted cluster (SAC)/SAC-CI method.

In the previous work,[13] we have analyzed the valence photoelectron and UV-visible absorption spectra of leuco dyes as used in heat-sensitive recording systems by the hydrogenic atoms in molecules (version 3) (HAM/3) MO[14] calculations. This procedure has an advantage over other methods in that the results can be directly compared with experiment without energy axis correction, because it uses the idea of Slater's transition-state[15] to predict vertical ionization potentials (VIPs). The calculated one hundred-six VIPs of twenty-five small molecules have an absolute deviation of 0.4 eV from experiment.[16,17] In contrast, VIPs predicted by Koopmans' theorem are too high, by approximately 8%.[18]

Here, we did not use the HAM/3 program to simulate the UV-visible spectra of the symmetrical molecules. Since the HAM/3 method cannot handle excitations from degenerate orbitals to degenerate orbitals properly,[16] corrections must be made by hand. Consequently, no configuration interaction computations of the symmetrical molecules have been carried out. Recently in the configuration interaction (CI) calculation, Pearl and co-workers[19] analyzed UV-visible absorption spectra of benzene, pyridine, pyrimidine, and pyridazine using ZINDO program.[20] The ZINDO calculations of the vacuous spectra for monosubstituted benzenes

are used to predict the maximum absorption frequency in water with linear correlation coefficient squared of 0.941, although the difference between the observed and predicted maxima is not constant: The linear relation is given by ν_{obsd} (nm) = $17.893+0.8524\times\nu_{calc}$ (nm), where ν_{obsd} (nm) and ν_{calc} (nm) denote the calculated and observed maxima of absorption frequencies in nm, respectively. For example, the value of 287 nm for the calculated maxima of nitrobenzene becomes 262.5 nm as the observed value in water.

In the present paper, we performed the HAM/3 calculations to simulate the valence X-ray photoelectron spectra (XPS) of the four molecules. The theoretical valence XPS showed very good accordance with experimental results, since the HAM/3 calculations of model molecules are within an absolute deviation of 0.4 eV from experiment in isolated molecules. In order to clarify the electronic state of transitions for the visible spectra of DPPD, PQP, OEP, and PC, we used a semiempirical ZINDO program,[20] since it involves the alternative parameterization for UV-visible absorption spectra. In the case of PC, we simulated visible spectra of PC and protonated PC in gas phase and concentrated H_2SO_4 solution, respectively. Our simulation in H_2SO_4 solution showed good correspondence with the observed spectrum, allowing a detailed analysis of the spectrum.

Experimental

1. Materials. We used commercially available compounds (*N*, *N*′-diphenyl-1,4-phenylenediamine (DPPD) (Aldrich Chem. Co. No. 25, 741-9), *p*-quaterphenyl (PQP) (Aldrich Chem. Co. No. 29, 226-5), 2,3,7,8,12,13,17,18-octaethyl-21*H*,23*H*-porphyrin (OEP) (Tokyo Kasei Ind.), and 29*H*, 31*H*-phthalocyanine (PC) (Dainichiseika Color & Chemicals Mfg. Co., Ltd.).

2. X-Ray Photoelectron Spectra (XPS). The experimental photoelectron spectra of four molecules (DPPD, PQP, OEP, and PC) were obtained on a PHI 5400 MC ESCA spectrometer, using monochromatized Al $K\alpha$ radiation (1486.6 eV). The spectrometer was operated at 600 W, 15 kV, and 40 mA. A pass energy of 35.75 eV was employed for high-resolution scans in valence-band analysis in the range of 50 eV. The angle between the X-ray source and the analyzer was fixed at 45°. The spot size in the measurement was 3×1 mm^2.

The use of dispersion compensation yielded an instrumental resolution of 0.5 eV FWHM (full width at half-maximum) on the Ag 3d line. Multiple scan averaging on the multichannel analyzer was used for the valence band region due to a very low emission cross section. For four compounds, we used the pressed thin discs. Gold of 20 A thickness was deposited on the discs of the dye samples using an ion sputter unit (Hitachi E 1030) for the scanning electron microscope.

A low energy electron flood gun was used in order to avoid any charging effect on the surface of the sample. We used the Au 4f core level of the gold decoration film as a calibration reference. The C1s line positions of phenyl rings on the dyes could be fixed at 285.0 eV.

3. UV-visible Absorption Spectra. We obtained the UV-visible absorption spectra of three molecules (DPPD, PQD, and OEP) in chloroform solution using a Shimadzu UV-3100 spectrometer at room temperature (25 °C). The molar ratio of DPPD and PQD sample solutions was adjusted to 1.0×10^{-5}, for the solution of OEP, the sample solution contained 3.8×10^{-6} M molecule (1 M = 1 mol dm^{-3}) in chloroform. In the case of PC, the sample solution contained 4.5×10^{-5} M in concentrated H_2SO_4 (95%) at room temperature.

Practical Details of MO Calculations

The electronic structures of the molecules (DPPD, PQD, OEP, and PC) for valence XPS were calculated by a new version of the HAM/3 program extended by Chong.[21] For the VIPs of the valence regions, we used the so-called diffuse ionization (DI) model which Asbrink and co-workers[14] proposed. In the restricted diffuse ionization (rDI) model, half of an electron is removed evenly from the valence MOs and the negative of the resulting orbital energies correspond to calculated VIPs. This allows us to obtain all the valence VIPs in a single calculation.

For the calculations of UV-visible spectra, the electronic states of the molecules were obtained using the configuration interaction calculations in ZINDO program. In the case of the geometry of the conductive molecules, we used the cartesian coordinates optimized with the semiempirical AM1 (version 6) method.[22] In the calculation of these molecules, we obtained the optimizing geometry with the dielectric constant (100 at 20 °C) of 95% H_2SO_4 and 4.9 of chloroform at 20 °C for COSMO option in MOPAC software, to reflect the solvent effect. Obtained point groups of DPPD, PQP, OEP, PC, and protonated PC by AM1 calculations were C1, D2, C1, D2h, and C1, respectively.

For the comparison between calculations for molecules in vacuum and experiments on solid or in solution, we must shift each computed energy value E_k' by a quantity σ, as $E_k = E_k' - \sigma$, to convert to ionization energy E_k relative to the Fermi level on solid, and to take account of solvent effect and other energy effects. The quantity σ on solid corresponds to WD[23–25] which denotes the sum of the work function and other energy effects (polarization energy and so on). The intensity of the photoelectron was estimated from the relative photoionization cross section for Al $K\alpha$ radiation using Gelius intensity model.[26] For the relative atomic photoionization cross section, we used the theoretical values from Nefedov et al.[27] as the computer output in the HAM/3 program.

The valence XPS and UV-visible absorption spectra of the molecules were simulated by the superposition of a peak centered on the shifted energy values, E_k. Each peak shape is represented by a Gaussian lineshape function:

$$F(x) = A(k)\ \exp\{-B(k)(x - E_k)^2\} \quad (1)$$

where the intensity, $A(k)$, is estimated from the relative photoionization cross section of Al $K\alpha$ radiation for the valence XPS and the transition probabilities for the UV-visible absorption spectra, respectively. For $B(k)$, we use the linewidth 0.10 E_k for the valence XPS, and a constant linewidth of 0.003 eV for the UV-visible spectra, respectively.

Results and Discussion

It is interesting that we can observe the characteristic spectra due to the photoionization cross section and oscillator

strength of any contributing molecular orbitals of constituent elements of the functional groups, respectively, for valence XPS and UV-visible absorption spectra. For these conductive molecules, we will clarify the orbital nature of the fingerprint spectra for the constituent elements in the range of 0—30 eV and 300—700 nm for photoelectron and UV-visible absorption spectra, respectively, from MO calculations using the single model molecules.

(a) Valence XPS of DPPD and PQP. Experimentally, we obtained similar valence spectra of DPPD and PQP, as obtained by Beamson and co-worker[28] (Figs. 1a and 1b). In Fig. 1, the simulated spectra of DPPD and PQP with the spectral patterns show excellent agreement with the observed ones. Then, we are able to analyze the electronic states of the molecules. For DPPD (in Fig. 1a), the four intense peaks at around 24, 20, 18, and 13 eV correspond to molecular photoionization cross sections from sσ(C2s-N2s, C2s)-, sσ(C2s-C2s)-, s,pσ(C2s-C2s, 2p)-, and {pσ(C2s-N2p, C2p)-, and pπ(C2p-C2p, N2p)-} bonding orbitals, respectively. The shoulder peaks between 3 and 12 eV are due to photoionization cross-section from pπ(C2p-C2p, N2p)-bonding orbitals.

For DPPD and PQP (in Figs. 1a and 1b), the intense peaks at around 18 eV are mainly due to the C2s photoionization cross section which results from sσ(C2s-C2s)-bonding orbital. In the case of PQP (in Fig. 1b), the three intense peaks in the energy range of 11—22 eV result from molecular photoionization cross section from sσ(C2s-C2s)-, pσ(C2s-C2p)-, and pπ(C2p-C2p)-bonding orbitals of benzene rings. The flat and shoulder peaks at around 9, 7, and 4 eV are due to pπ(C2p-C2p)-bonding orbital. The WDs of DPPD and PQP between observed and calculated VIPs were estimated as 5.1 and 4.0 eV, respectively. We showed observed VIPs, main atomic orbital photoionization cross section, and orbital nature of PQP in Table 1 (For DPPD, we omitted a similar table). The orbital nature and functional group mean the contribution to each peak of the photoelectron spectra.

(b) Valence XPS of OEP and PC. In Figs. 2a and 2b, the theoretical valence spectra of OEP and PC were compared with the observed valence XPS. The simulated spectra showed fairly good agreement with observed spectra. For OEP (in Fig. 2a), both the skirt region between 24 and 28 eV and the intense peak at around 20 eV are owing to sσ(C2s-C2s, N2s)-bonding orbital. The peak at around 17 eV is due to sσ(C2s-C2s)-bonding orbital. The WD was evaluated as 4.1 eV for OEP. In Table 2, we showed observed VIPs, main atomic orbital photoionization cross section, and orbital nature of the OEP molecule.

In the case of PC (in Fig. 2b), three broad peaks at around 23, 19, and 15 eV correspond to photoionization cross sections from sσ(C2s-C2s, C2s-N2s)-bonding orbitals. Other peaks at around 6 and 12 eV for PC correspond to the similar ones (at around 6 and 11 eV) for OEP. These are due to the C2s, C2p, N2p photoionization cross sections which result from pσ, pπ(C2s-C2p, N2p; C2p-C2p, N2p)-bonding orbitals, and pπ(C2p-C2p, N2p)-bonding orbitals, respectively, for PC and OEP molecules. Our observed peaks of PC molecules at around 6, 12, and 15 eV also correspond to the experimental peaks of PC in gas at around 6.4, 9.0, and 14

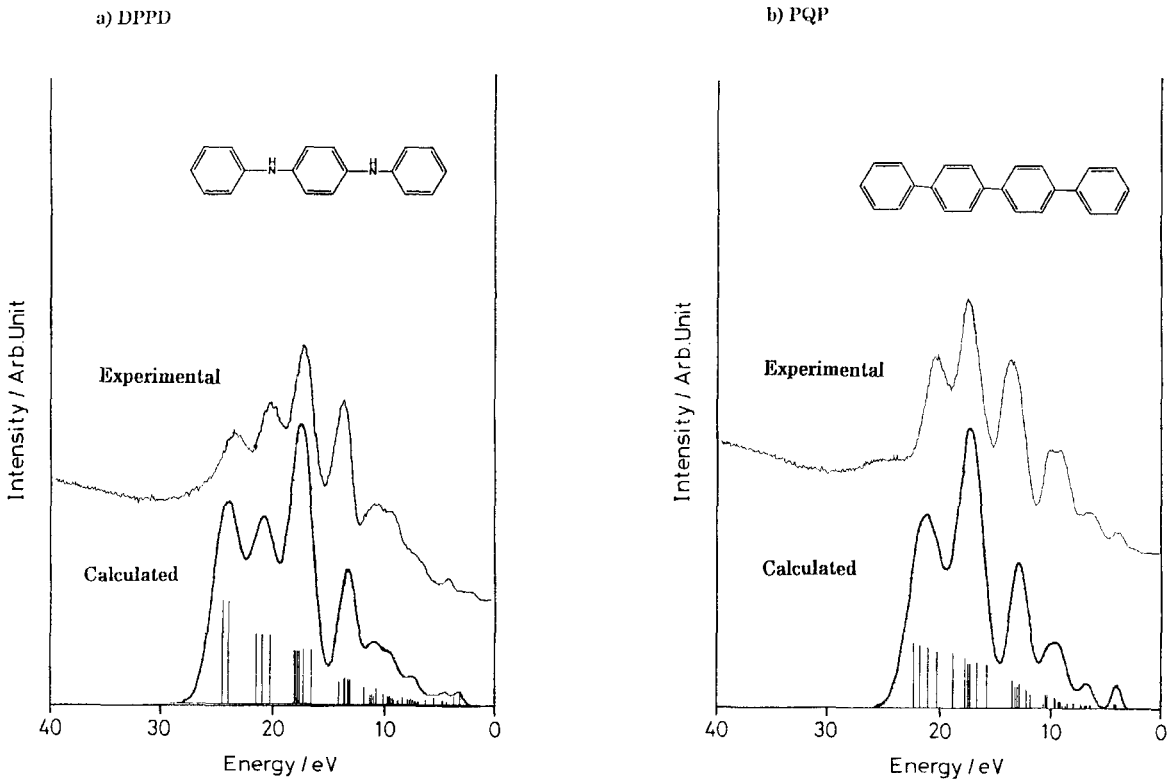

Fig. 1. a) Valence XPS of DPPD with the simulated spectra of the single molecule, and b) Valence XPS of PQP with the simulated spectra of the single molecule.

Table 1. Observed Peaks, VIP, Main AO PICS, Orbital Nature, and Functional Group for Valence XPS of PQP (The Gap between Observed and Calculated VIPs) = 4.0 eV

Peaks/eV	VIP/eV	Main AO PICS	Orbital nature[b)]	Functional group
21.0 (19—23)[a)]	27.1; 26.6; 25.8; 25.0	C2s	sσ(C2s-C2s)-B	C–C
18.0 (16—19)[a)]	22.0—23.6	C2s	sσ(C2s-C2s)-B	C–C
13.0 (11—15)[a)]	17.5—18.1	C2s, C2p	s,pσ(C2s-C2s,C2p)-B	C–C=C
9.0 (8—11)[a)]	12.5—16.8	C2p	pπ(C2p-C2p)-B	C=C
7.0 (5—8)[a)]	11.0—11.9	C2p	pπ(C2p-C2p)-B	C=C
4.0 (3—5)[a)]	8.6—8.8	C2p	pπ(C2p-C2p)-B	C=C

a) Shows the peak range. b) B means bonding. (C2s-C2s,C2p) means (C2s-C2s) and (C2s-C2p).

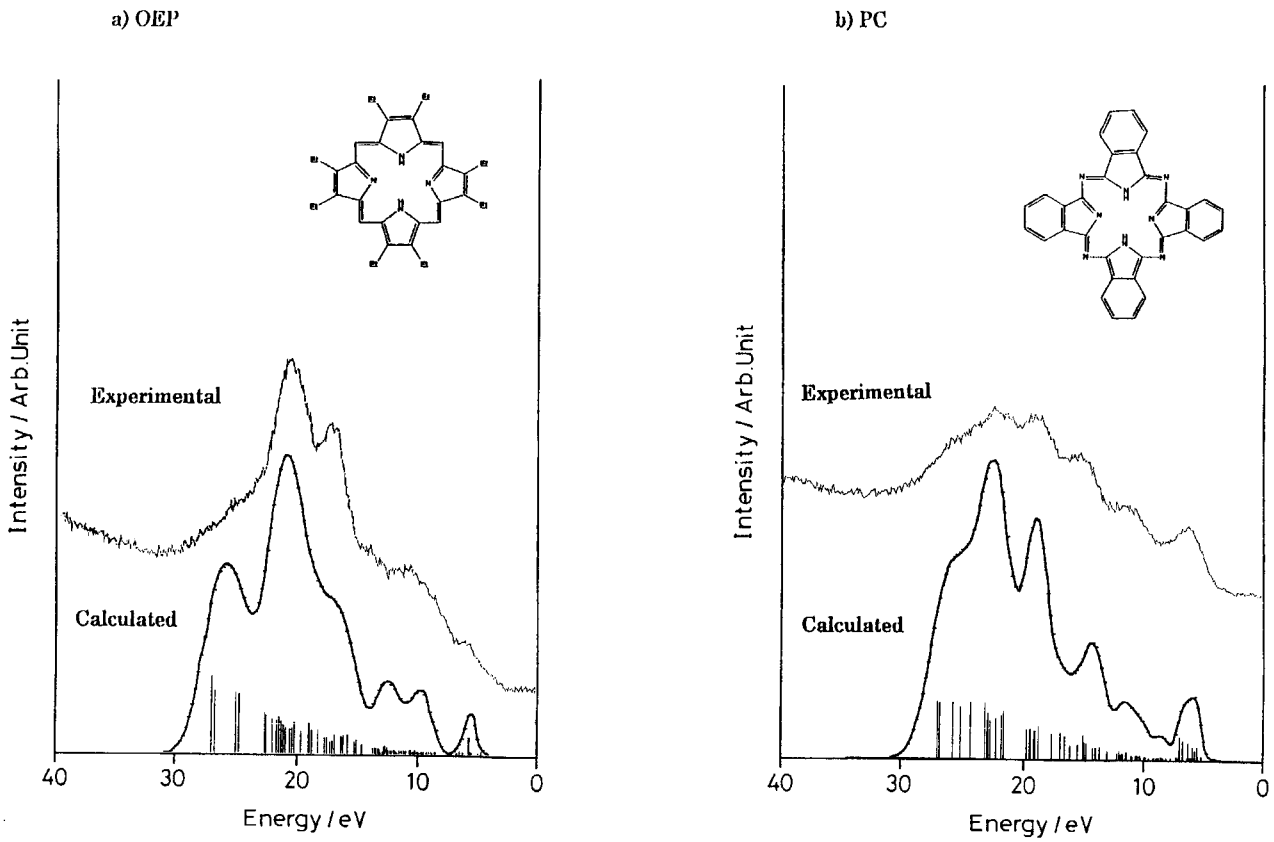

Fig. 2. a) Valence XPS of OEP with the simulated spectra of the single molecule, and b) Valence XPS of PC with the simulated spectra of the single molecule.

eV, respectively, as obtained in UPS.[8] For the experimental values in the gas phase we can state that the phthalocyanine in gas phase is not a isolated molecule, but an oligomer, since the VIPs using the single model molecule were estimated as 9.0—11.5, 13.5—16.0, and 16.5—22.0 eV. In Table 3, we showed the observed peaks, VIPs, main AO photoionization cross section, and orbital nature of PC. The WD value was estimated as 4.0 eV for PC.

(c) UV-visible Spectra of Four Molecules. In order to simulate the UV-visible spectra, we used the method of configuration interaction for DPPD and PQP in ZINDO program. The energies at the high intensities of the molecules were selected from the output of the calculation. For a best fit of simulated spectra with observed ones (Figs. 3a and 3b), we shifted the energy levels with 0.20 eV for DPPD and PQP molecules. In the middle of Figs. 3a and 3b, we showed the MO diagram of the transitions for absorption spectra of DPPD, to clarify the orbital nature. For DPPD, the absorption spectrum results from the excitation between the π-bonding HOMO (π-electrons which conjugated in phenylene ring in the center) and the π*-antibonding LUMO (π*-electrons which conjugated in the phenyl ring at the left hand). For

Table 2. Observed Peaks, VIP, Main AO PICS, Orbital Nature, and Functional Group for Valence XPS of OEP (The Gap between Observed and Calculated VIPs) = 4.1 eV

Peaks/eV	VIP/eV	Main AO PICS	Orbital nature[b)]	Functional group
Shoulder	{30.3; 30.0	C2s(0.5), N2s(0.5)	sσ(C2s-C2s,N2s)-B	C–C, C–N
(24–28)[a)]	28.3; 28.0}	C2s(0.7), N2s(0.3)	sσ(C2s-C2s,N2s)-B	C–C, C–N
20.0	21.2—25.8	C2s	sσ(C2s-C2s)-B	C–C
(18–13)[a)]	(21.9)	C2s, C2p, N2s	s,pσ(C2s, C2p-C2s,N2s)-B	C–C, C–N
17.0	{17.6—20.7	C2s	sσ(C2s-C2s)-B	C–C
(15–18)[a)]	19.9	C2s, N2p	pσ(C2s-N2p)	C–N–C
	18.8; 18.0	C2s, N2p	pσ(C2s-N2p)	C–N
	16.3—16.9}	C2s, C2p, N2p	s,pσ(C2s-C2s, C2p, N2p)-B	C–N, C–C
13.5	14.1—16.6	C2p, N2p	pπ(C2p-C2p, N2p)-B	C=C, C=N
(12–15)[a)]	(15.8)	C2s, C2p,	pσ(C2s-C2p)-B	C–C
11.0	10.0—13.9	C2p	pπ(C2p-C2p)-B	C=C
(8–12)[a)]	{13.1; 13.0; 11.8; 11.7}	C2p, N2p	pπ(C2p-C2p, N2p)-B	C=C, C=N
6.0	{9.7—8.4	C2p	pπ(C2p-C2p)-B	C=C
(5–7)[a)]	8.3; 7.8	C2p, N2p	pπ(C2p-C2p, N2p)-B	C=C, C=N
	7.5}	N2p	pπ(lone pair)-NB	–N–

a) Shows the peak range. b) B means bonding. (C2s-C2s, N2s) means (C2s-C2s) and (C2s-N2s).

Table 3. Observed Peaks, VIP, Main AO PICS, Orbital Nature, and Functional Group for Valence XPS of PC (The Gap between Observed and Calculated VIPs) = 4.0 eV

Peaks/eV	VIP/eV	Main AO PICS	Orbital nature[b)]	Functional group
Shoulder	{30.1; 29.9	C2s(0.5), N2s(0.5)	sσ(C2s-C2s,N2s)-B	C–C, C–N
(24—28)[a)]	28.8; 28.1}	C2s(0.6), N2s(0.4)	sσ(C2s-C2s,N2s)-B	C–C, C–N
23.0	{27.3	C2s(0.4), N2s(0.6)	sσ(C2s-N2s)-B	C–N
(21—24)[a)]	26.1; 24.6	C2p, N2s	pσ(C2p-N2s)-B	C–N
	26.0; 25.7; 25.2	C2s	sσ(C2s-C2s)-B	C–C
	25.9; 24.8}	C2s, C2p, N2p	pσ(C2s-C2p, N2p)-B	C–N
19.0	{22.6—22.0	C2s	sσ(C2s-C2s)-B	C–C
(18—21)[a)]	21.6	C2s, N2p	s,pσ(C2s-C2s, N2p)-B	C–C, C–N
	20.5; 19.8	C2s,C2p,N2s,N2p	pσ(C2s-N2p;C2p-N2s)-B	C–N
	19.0; 18.3}	C2s,C2p,N2p	s,pσ(C2s-C2s,N2p)-B	C–C, C–N
15.0	{17.0—17.9	C2s,C2p,N2s,N2p	pσ(C2s-N2p;C2p-N2s)-B	C–N
(13—16)[a)]	15.9—17.0}	C2s,C2p,N2s,N2p	{s,pσ(C2s-C2s;C2s-C2p, N2p)-B,	C–C
			pπ(C2p-N2p)-B}	C=N
12.0	10.5—15.0	{C2p,N2p	pπ(C2p-C2p,N2p)-B	C=C, C=N
(9—13)[a)]		C2p}	pπ(C2p-C2p)-B	C=C
6.0	{8.2—10.0,	C2p, N2p	pπ(C2p-C2p,N2p)-B	C=C, C=N
(5—9)[a)]	7.9,	N2p	pπ(lone pair)-NB	–N–
	6.9}	C2p	pπ(C2p-C2p)-B	C=C

a) Shows the peak range. b) B means bonding. (C2s-C2s, N2s) means (C2s-C2s) and (C2s-N2s), and [(C2s, C2p-N2p), (C2p-N2s)] denotes (C2s-N2p), (C2p-N2p), and (C2p-N2s) and so on.

PQP (we omitted the MO diagram), the absorption spectrum corresponds to the transition from the π-bonding HOMO (which is due to π-electrons in two benzene rings at the left hand) to the π^*-antibonding LUMO of two benzene rings in the middle of four rings.

In Fig. 4, we observed the intense peak as Soret Band or B-band at around 390 nm with shoulder peak, and four additional weak peaks called Q-band for OEP. For a fit of the simulated spectrum with the observed weak peak at around 620 nm, we shifted the energy level with 0.20 eV. The simu-

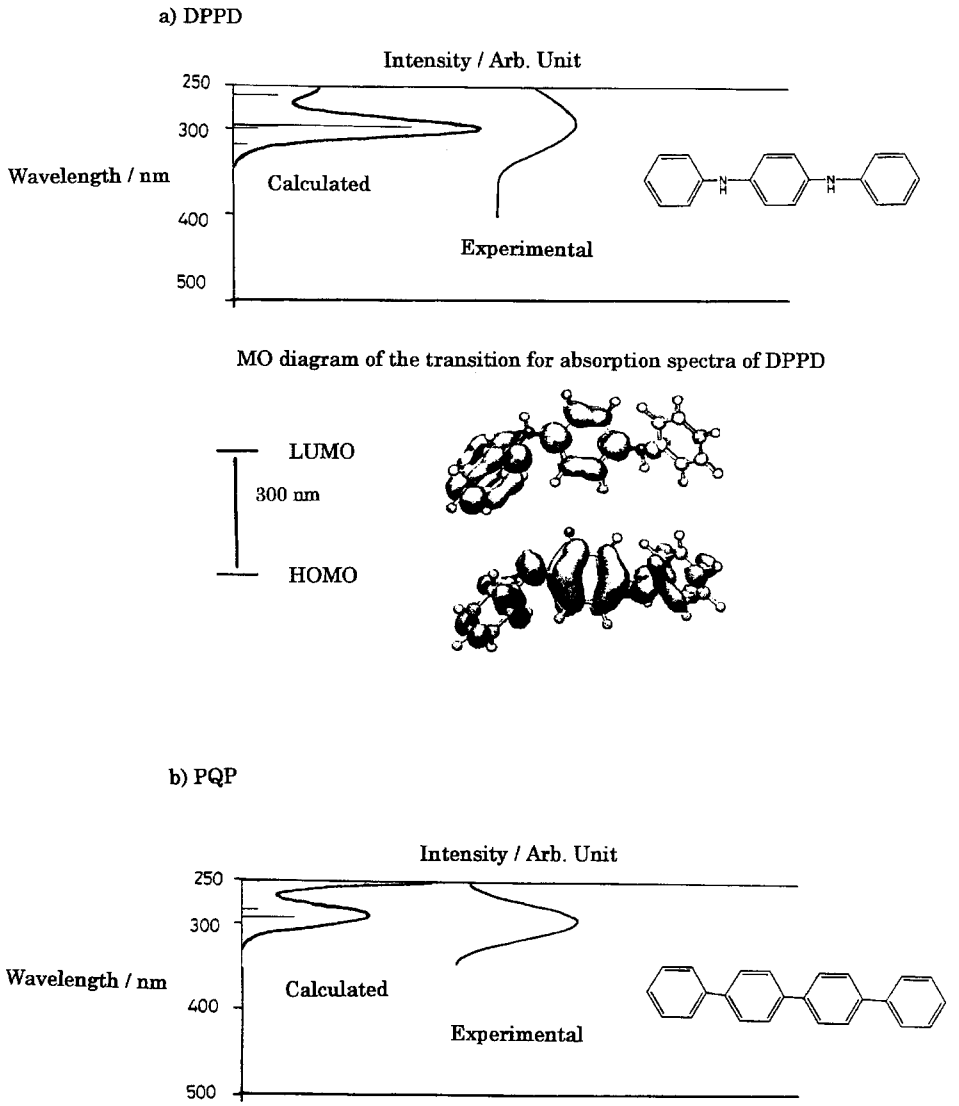

Fig. 3. a) UV visible absorption spectra of DPPD with the simulated spectra of the single molecule; MO diagram of the transition for absorption spectra of DPPD using the method of configuration interaction for single molecule in ZINDO program, and b) UV visible absorption spectra of PQP with the simulated spectra of the single molecule.

lated peaks at around 300 and 390 nm are in good accordance with observed ones at B band, although the experimental four weak peaks at the Q-band were not sufficiently reproduced with two simulated peaks. The MO diagram of the main transitions is shown in the lower part of Fig. 4. The simulated peaks (620 and 580 nm) of Q-band are due to the excitations from the π-bonding HOMO to the π^*-antibonding LUMO, and to the π^*-antibonding next LUMO, respectively. The intense peak of B-band is owing to the transitions (395 and 390 nm) from the π-bonding next HOMO to the LUMO, and to the next LUMO, respectively.

For PC, the two Q-bands of absorption spectra in vapor were observed as Qx at 686 nm and Qy at 622.5 nm by Edward and co-worker.[9] These values correspond to 954 and 821 nm for Qx and Qy in the reference,[12] respectively. As obtained with optimizing geometry without COSMO option by our CI calculation using ZINDO program, our calculated values (664 and 656 nm for Qx and Qy) correspond to those observed by Edward and co-worker,[9] respectively.

In Figs. 5a, 5b, and 5c, we showed the three simulated absorption spectra for two types of protonation (a) or b) means inner- or outer-protonation (IP or OP) for PC-ring. IP and OP correspond to protonated pyrrole aza and mesobridging aza nitrogens, respectively, as indicated in reference[10]) and the mixed type of protonation (c) consists of 0.5 IP and 0.5 OP types). The MO diagram for protonated PCs was omitted here. We emphasize that the mixed spectrum shows much better agreement with the experimental one than the spectrum of either IP or OP type alone.

In Table 4, we listed calculated excitation energies of PC and protonated PC in Q bands along with the observed ones. We shifted the energy level with 0.19 eV to fit the simulation with the observed peak at around 844 nm. Our simulation of the PC and protonated PC using the ZINDO/AM1 methods showed good correspondence with the observed ones, allowing a detailed analysis of the spectra.

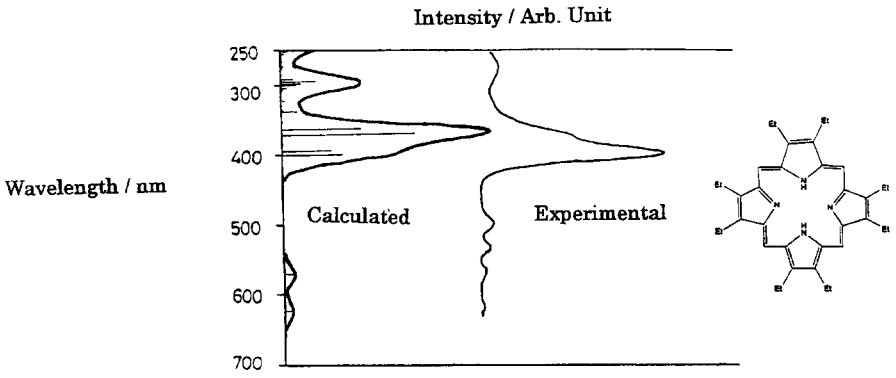

MO diagram of the transitions for absorption spectra of OEP

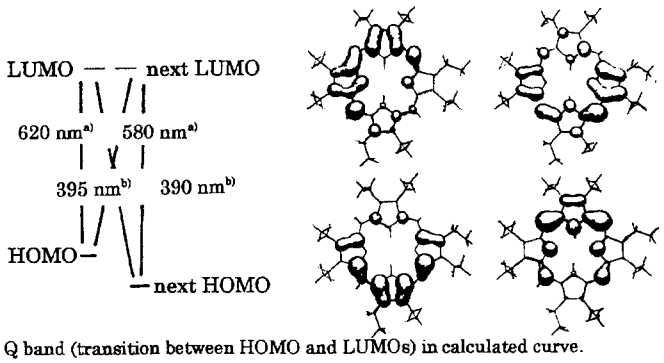

a): Q band (transition between HOMO and LUMOs) in calculated curve.

b): Soret Band (transition between next HOMO and LUMOs) in calculated curve.

Fig. 4. UV visible absorption spectra of OEP with the simulated spectra of the single molecule; MO diagram of the transition for absorption spectra of OEP using the method of configuration interaction for single molecule in ZINDO program.

Table 4. Calculated Peaks Using ZINDO/AM1 and Observed Q-Bands of PC in Gas Phase and 95% H_2SO_4

Calculated peak nm and eV	Observed peak nm and eV	Assignment due to model molecule
	In gas phase[a]	
664 1.87 (954 1.30)[b]	686 1.81	Qx
656 1.89 (821 1.51)[b]	622 1.99	Qy
	In 95% H_2SO_4	
844 1.47[c]	847 1.46	Qx of OP
817 1.52[c]	780 1.59	Qx of IP
752 1.66[c]	746 1.65	Qy of IP
696 1.93[c]	644 1.78	Qy of OP

a) Values were referred to Ref. 9. b) Values were referred to results[12] obtained by SAC and SAC/CI methods. c) Values were shifted with 0.19 eV to fit the simulation with the observed peak at around 844 nm.

For a comparison between calculations for single molecules and experiments in solution, we must shift each computed energy levels E'_k by a quantity σ, as $E_k = E'_k - \sigma$. When the quantity σ is assumed to be due to the solvent effect, the polar solvent effects of chloroform or H_2SO_4 for four compounds were estimated as 0.19 to 0.20 eV. This means that chloroform or H_2SO_4 causes a red shift to the compounds, if we can consider $\sigma E_{\pi\to\pi^*}$ (vacuum) $> \sigma E_{\pi\to\pi^*}$ (solution) for the difference of the transition energies in vacuum and polar solutions between HOMO and LUMO of the compounds, respectively.

Conclusion

We have analyzed the valence XPS and UV-visible absorption spectra of four molecules (DPPD, PQP, OEP, and PC) by a semiempirical HAM/3 and ZINDO calculations using the single molecules, respectively. The present results suggest several new analytical aspects of the electron spectra:

(1) The HAM/3 method can be used to provide better assignment of the valence XPS of the molecules involving carbon, nitrogen, and oxygen. The Fermi levels of these compounds are evaluated as −5.1, −4.1, and −4.0 eV for

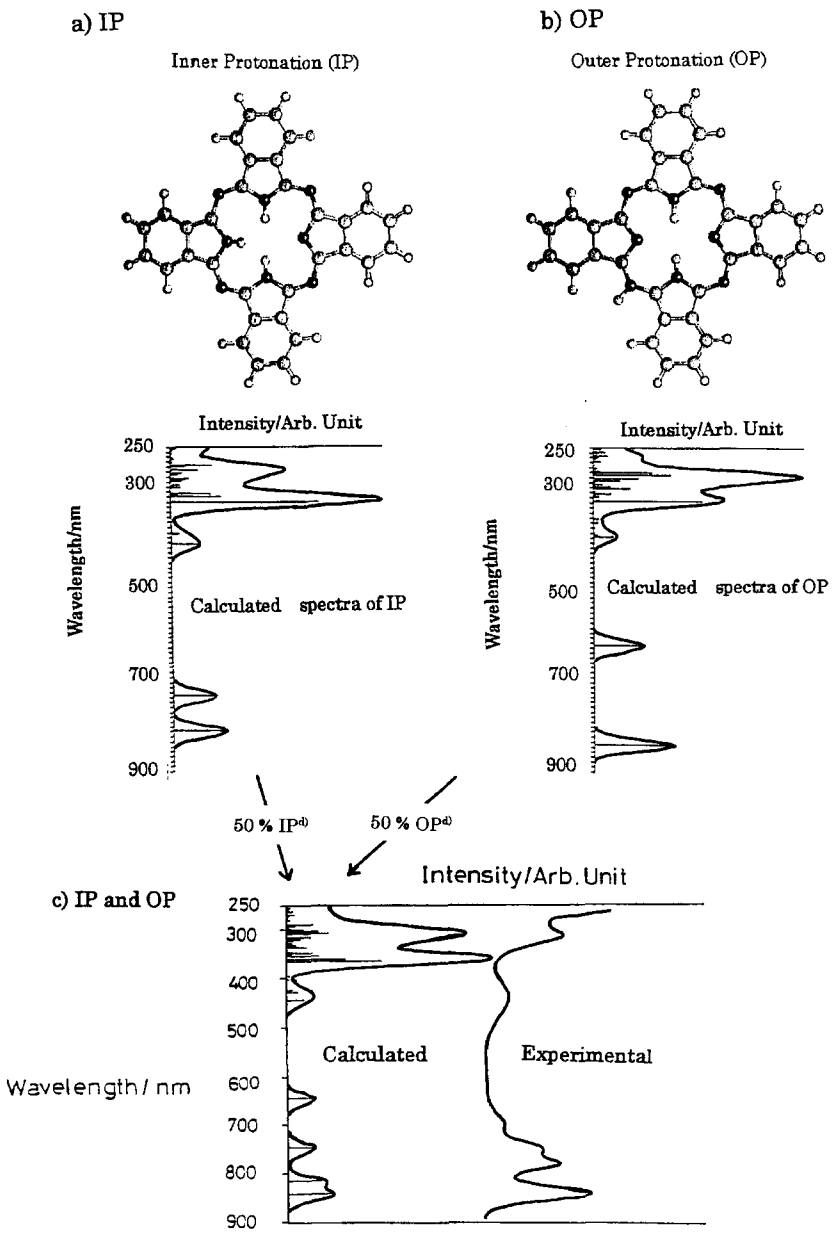

d) Calculated values of Heat Formation for IP and OP are 1990 and 2000 kJ, respectively, by AM1 program.

Fig. 5. a) The simulated spectra of inner protonation (IP), b) The simulated spectra of outer protonation (OP), and c) UV visible absorption spectra of PC with the simulated spectra of mixed type of protonation consisted of 0.50 IP and 0.50 OP type.

DPPD, OEP, and (PQP, PC), respectively, from the comparison between calculations of molecules in vacuum and experiments on solid.

(2) We were able to analyze the electronic states of transition for visible absorption spectra for four conductive molecules using the method of configuration interaction for single molecules in ZINDO program. Furthermore, we can state that the solvents cause a red shift to the molecules, if we can consider $\delta E_{\pi\to\pi^*}$ (vacuum) > $\delta E_{\pi\to\pi^*}$ (solvent) for the difference of the excitation energies in vacuum and polar chloroform or H_2SO_4 solution between HOMO and LUMO of four molecules, respectively.

(3) We were able to explain that the Q-bands in PC in 95% H_2SO_4 appeared in the region of 650—850 nm on the assumption of two types of protonated PCs (IP and OP). In this assumption, the first strong peak at 850 nm and the second peak of 780 nm are owing to Qx-bands of OP and IP types, respectively, while the peaks at around 750 and 650 nm are due to Qy-bands of IP and OP, respectively.

References

1 M. E. Vaschetto and B. A. Retamal, *J. Phys. Chem.*, **101**, 6945 (1997).

2 K. G. Neoh, E. T. Kang, and K. L. Tan, *J. Phys. Chem.*, **96**, 6777 (1992).

3 R. K. Khanna, Y. M. Jiang, B. Srinivas, and C. B. Smithhart, *Chem. Mater.*, **5**, 1792 (1993).

4 A. Kawaski, G. Piszczk, and A. Kubicki, *Z. Naturforsch. Sect. A-A, J. Phys. Sci.*, **51**, 905 (1996).

5 Y. Kaneda, Y. Takagami, Y. Aizawa, and T. Senga, "The 9th International Congress on Advances in Non-Impact Printing Technologies/Japan Hardcopy '93," Abstr., Oct7-II-a3.

6 M. Bossa, E. Cervone, C. Garzillo, and G. Del Re, *J. Mol. Struct.*, **342**, 73 (1995).

7 D. Dolphin, "The Porphyrins," Academic Press, London (1998), Vols. 1—7.

8 J. Berkowitz, *J. Chem. Phys.*, **70**, 2819 (1979).

9 L. Edwards and M. Gouterman, *J. Mol. Spectrosc.*, **33**, 292 (1970).

10 E. Orti, L. Bredas, and C. Clarisse, *J. Chem. Phys.*, **92**, 1228 (1990).

11 N. Kobayashi and H. Konami, "Phthalocyanines-Properties and Applications," VCH, Weinheim (1996), p. 4.

12 K. Toyota, J. Hasegawa, and H. Nakatsuji, *J. Phys. Chem. A*, **101**, 446 (1997).

13 K. Takaoka, S. Maeda, H. Miura, K. Endo, and D. P. Chong, *Bull. Chem. Soc. Jpn.*, **71**, 807 (1998).

14 L. Asbrink, C. Fridh, and E. Lindholm, *Chem. Phys. Lett.*, **52**, 63(1977); *Quantum Chem. Program Exch.*, **12**, 398 (1980); L. Asbrink, C. Fridh, and E. Lindholm, *Chem. Phys. Lett.*, **52**, 69 (1977); E. Lindholm and L. Asbrink, "Molecular Orbitals and Their Energies, Studied by Semiempirical HAM Method," Springer-Verlag, Berlin (1985).

15 J. C. Slater, *Adv. Quantum Chem.*, **6**, 1 (1972).

16 D. P. Chong, *Can. J. Chem.*, **58**, 1687 (1980).

17 P. Duffy and D. P. Chong, *Org. Mass Spectrom.*, **28**, 321 (1993)

18 M. E. Schwartz, in "Application of Electronic Structure Theory," 3rd ed, ed by H. F. Schaefer, Plenum, New York (1987).

19 G. M. Peary, M. C. Zerner, A. Broo, and J. Mckelvey, *J. Comput. Chem.*, **19**, 781 (1998).

20 "ZINDO, A Semiempirical Quantum Chemistry Program," ed by M. C. Zerner and co-workers, University of Florida, Gainesville, FL, distributed by MSI Technologies, San Diego, CA, www.msi.com.

21 D. P. Chong, *Can. J. Chem.*, **63**, 2007 (1985).

22 M. J. S. Dewar and E. G. Zoebisch, *Theochem.*, **180**, 1 (1988); M. J. S. Dewar, E. G. Zoebisch, E. F. Healy, and J. J. P. Stewart, *J. Am. Chem. Soc.*, **107**, 3902 (1985).

23 K. Endo, C. Inoue, Y. Kaneda, M. Aida, N. Kobayasi, and D. P. Chong, *Bull. Chem. Soc. Jpn.*, **68**, 528 (1995).

24 K. Endo, Y. Kaneda, M. Aida, and D. P. Chong, *J. Phys. Chem. Solids*, **56**, 1131 (1995).

25 K. Endo, Y. Kaneda, H. Okada, D. P. Chong, and P. Duffy, *J. Phys. Chem.*, **100**, 19455 (1996).

26 U. Gelius and K. Siegbahn, *Faraday Discuss. Chem. Soc.*, **54**, 257 (1972); U. Gelius, *J. Electron Spectrosc. Relat. Phenom.*, **5**, 985 (1974).

27 V. I. Nefedov, N. P. Sergushin, I. M. Band, and M. B. Trzhaskovskaya, *J. Electron Spectrosc. Relat. Phenom.*, **2**, 383 (1973).

28 G. Beamson and D. Briggs, "High Resolution XPS of Organic Polymers, The Scienta ESCA 3000 Database," Wiley, Chichester (1992).